SPECTRAL ANALYSIS OF THE HIMAWARI-8 DATA FOR HOTSPOT DETECTION FROM LAND/FOREST FIRES IN SUMATRA

Hana Listi Fitriana[1], Sayidah Sulma, Any Zubaidah, Suwarsono, and Indah Prasasti
Remote Sensing Applications Center, LAPAN
Jl. Kalisari No.8, Pekayon, Pasar Rebo, Jakarta Timur, Indonesia
[1]e-mail: hana.listi@lapan.go.id

Received: 8 November 2017; Revised: 3 June 2018; Approved: 22 June 2018

Abstract. Himawari-8 is the last generation of the low spatial resolution satellite imagery that has capability to detect the thermal variation on the earth of every 10 minute. This must be very potential to be used for detecting land/forest fire. This paper has explored the spectral prospective of the Himawari-8 for detecting land/forest fire hotspot. The main objective for this study is to identify the potential use of Himawari-8 for detecting of land forest fire hotspot. The study area was performed in Ogan Komering Ilir, South of Sumatra, which on 2015 occur great forest/land fire event. The main process included in this study are image projection, training sample collection and spectral statistical analysis measured by calculate statistic, they are average values, standard deviation values from reflectance visible band value and brightness temperature value, beside that validation of data obtained from medium resolution data of Landsat 8 with the similar acquisition time. The study found that the Himawari-8 has good capacity to identify land/forest fire hotspot as expressed for high accuracy assessment using band 3 and band 7.

Keywords*: Himawari-8, hotspot, spectral*

1 INTRODUCTION

Land/forest fires are frequent and recurring natural phenomenon every year in Indonesia, particularly in Sumatra and Kalimantan during the dry season. However, forest and land fires have international the environmental and economic issue, specifically after the 1997/1998 El Nino (ENSO) disaster which burned 25 million hectares of forest and land worldwide (Tacconi 2003). The disaster has been perceived as a potential threat to establishment continuing because of its direct impact on ecosystems, its contribution to carbon emissions and their impacts on degradation of biodiversity (Tacconi 2003). From the aspect of population activity and public health, it was obviously that the forest and land fires have the worst effect of the daily healthy activities, especially respiratory disorders (Frankenberg 2005). The smoke caused by forest and land fires provoked the political problems of among neighboring country of transboundary haze, as the case in Southeast Asia (Murdiyarso 2004).

In Indonesia, hotspot data had contributed a very significant role in monitoring the potential accuracy of land/forest fires. The hotspot data distribution has been required of both land/forest fire prevention and suppression for minimize the effect of widespread land fires. Hotspot information that is often used today is mostly processed from polar sensor satellite data, such as MODIS-Terra/Aqua, ERS-ATSR, NOAA-AVHRR, and SNPP-VIIRS. From several sources of data, MODIS is the most

http://dx.doi.org/10.30536/j.ijreses.2018.v15.a2836

popular, although the Terra/Aqua satellite carrying them MODIS sensor will end its life time which will be completely replaced by VIIRS. The data that is generated by satellite polar sensor recording has a disadvantage, namely the second of limited period, despite of having sufficient spectral and spatial capability to monitoring the hotspot. Satellites are passing through the same area of the earth a day only a few times, in other words 2 times a day. This condition might cause a fire at the interval of the two recording which will not be monitored by polar satellite. Beside that mission of the MODIS satellite will be over soon after launched 6 years ago, in the transition period required to explore geostationary for detecting hotspot. Therefore, to overcome this condition, the use of geostationary data will be able to provide a solution because of its more real time of recording capability. However, the previous geostationary satellites (prior to the presence of Himawari-8), were not used to monitoring the hotspots. This condition is due to limited spatial resolution. By the existence of Himawari-8, which has a higher radiometric, more spectral, and spatial resolution higher than MTSAT, coupled with faster recording periods, this data has the potential to monitor hotspots.

Himawari-8 has 16 channels that include visible, near infrared and infrared channels with spatial resolution of 500 meters, 1 km and 2 km. Himawari-8/AHI has another advantages, it is capable to recording with a much better repeat period around 2.5 minutes to 10 minutes. With these capabilities, the data will be the best of observing the object or phenomena which have dynamics and rapid changed, such as clouds, rain, wind, the dust particle, volcanic ash, until phenomenon of forest and land fires.

This study aims to identify the potential utilization of Himawari-8 data for hotspot detection. This research is a preliminary study aimed at understanding the spectral of characteristics for the development of model hotspot information extraction from Himawari-8 data.

2 MATERIAL AND METHODOLOGY

2.1 Study Site

The location is part of Sumatra, which covered by Landsat-8 satellite coverage for path/row 123/062 (Figure 1-1). The area of Ogan Komering Ilir is located in the eastern part of South Sumatera Province which is precisely between 104 ° 20 'and 106 ° 00' East Longitude and 2 ° 30 'to 4 ° 15' South Latitude, the area reaches 19,023.47 km².

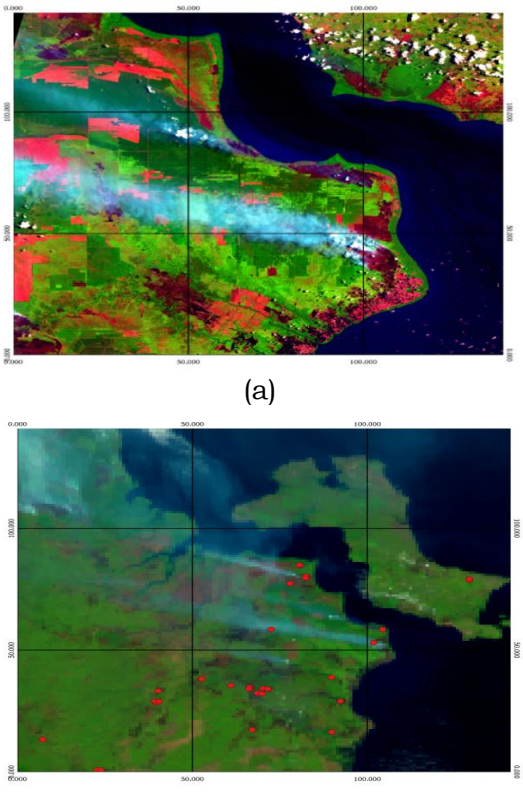

(a)

(b)

Figure 1-1: Ogan Komering Ilir District Map, South Sumatera (a) Landsat-8 path / row 123/062, (b) Himawari-8 with Hotspot from MODIS data on September 23, 2015

2.2 Data

Data used in this Study was Himawari-8 data obtained from Japan Meteorological Agency (JMA) through Himawari Cloud at website address http://www.jma.eorc.jaxa.jp. Himawari-8 data used is data of recording on

September 23, 2015 acquisition at 10.00 am and landsat-8 path/row image 123/062 on that date there was a big fire in the region. The format data used is the Network Common Data Field (NetCDF). As it is known that the revisit time of this data is 10 minutes, here is the selection of the recording time becomes necessary to pay attention, (Wickramasinghe 2016), that conducts the research in the Australian region, selected the recording time at 09.00 am to 4.00 pm. Compared with MODIS data, Himawari data excellence is in temporal resolution, which can be seen in the Table 2-1.

The others supporting data used are hotspot data from MODIS and Landsat-8 image. Study object is a hotspot on fire incident in Ogan Komering Ilir District, South Sumatera.

The hotspot detection from MODIS imagery used channels 21 or 22 and 31 (wavelengths 4 µm and 11 µm), where the hotspot detection method of MODIS data is based on algorithms that is built for AVHRR and TRMM VIRS image data (Giglio 1999; Justice 1996; Kaufman 1990, 1998, Justice 2002; Giglio 2003). It also uses red and near infrared channels to 250 m resolution to remove fake hotspots due to *sun glint* (Justice 2002). Considering of the channels which used to detect hotspots with MODIS data above, it can be seen that hotspots can be detected using 4 µm, 11 µm, 0.86 µm and 0.65 µm wavelengths. In the Himawari-8 / AHI data, the wavelength is in channel 7 (3.9 µm), 14 (11.2 µm), 4 (0.86 µm), and 3 (0.64 µm).

Channel 5, Channel 6 and Channel 7 reflectance variables in MODIS image data are among the best indicators in the detection of fired areas (Suwarsono 2013). Based on this matter, it is calculated the average reflectance value of Channels 3 and 4 and BT from Channels 7 and 14.

Table 2-1: Comparison of sensor characteristics of Himawari-8/AHI (Bessho *et al.* 2016) and MODIS Imager (https://modis.gsfc.nasa.gov/about/specifications.php)

Himawari-8/AHI			**MODIS**					
Band	**Wave length channel (µm)**	**Spatial Resolution (m)**	**Band**	**Wavelength channel (µm)**	**Spatial Resolu-tion (m)**	**Band**	**Wavelength channel (µm)**	**Spatial Resolu-tion (m)**
1	0.47	1000	1	0.62-0.67	250	19	0.915 –0.965	1000
2	0.51		2	0.84 – 0.88		20	3.660 – 3.840	
3	0.64	500	3	0.46 – 0.48		21	3.929 – 3.989	
4	0.86	1000	4	0.55 -0. 57		22	3.929 – 3.989	
5	1.6		5	1.23– 1.25	500	23	4.020 – 4.080	
6	2.3		6	1.63– 1.65		24	4.433 – 4.498	
7	3.9		7	2.105 – 2.155		25	4.482 - 4.549	
8	6.2		8	0.405 – 0.420		26	1.360 – 1.390	
9	6.9		9	0.438 – 0.448		27	6.535 – 6.895	
10	7.3	2000	10	0.483 – 0.493		28	7.175 – 7.475	
11	8.6		11	0.526 – 0.536		29	8.400 – 8.700	
12	9.7		12	0.546 – 0.556		30	9.580 – 9.880	
13	10.4		13	0.662 – 0.672	1000	31	10.780 – 11.280	
14	11.2		14	0.673 – 0.683		32	11.770 – 12.270	
15	12.4		15	0.743 – 0.753		33	13.185 – 13.485	
16	13.3		16	0.862 –0.877		34	13.485 - 13.785	
			17	0.890 –0.920		35	13.785 – 14.085	
			18	0.931 –0.941		36	14.085 – 14.385	

Taking into the effect of the daily cycles of land surface temperatures, where within a day of the maximum surface temperature occurs at mid-day, it is necessary to analyze the spectral pattern of near infrared, red, and infrared wavelength (Wickramasinghe *et al.* 2016). Therefore, Wickramasinghe *et al.* (2016) suggest that the average and standard or reflectance deviation should be calculated from 9 am to 2 pm for some land cover (urban settlements, vegetation, meadow, bare land and land fires).

2.3 Method

The method in this study include several step including data preparation, training sample collection, statistic spectral analysis of pixel hotspot and data validation.

a. Data Preparation

The Himawari-8 data recording every 10 minute, the format data used NetCDF were extracted, projected process used to change the geometry of Himawari-8 data to using georeference information and saved to GeoTIFF. MODIS data selected time at 10.00 am to extract the Hotspot information, were projected and saved to Shape file format.

The Landsat-8 data dated 0f 23 September 2015 selected for band 6, 5 and 4, then converted to reflectance value. After that the data was created to image RGB 654.

b. Training sample collection

Determination of hotspot pixel samples aids by higher spatial resolution that is Landsat-8 imagery and hotspot data distribution from MODIS to be studied for its characteristics. The Landsat-8 image that is chosen for this purpose is the recording date data corresponding to the Himawari-8 data used. Similarly MODIS hotspot data are selected with the appropriate date and time.

Training samples include land/forest fire, shrub, forest, urban settlement, bare land, plantation and water. Usually the object which has similar brightness temperature value with hotspot were urban settlement and bare land. The objects of training samples are shown in Figure 2-2.

c. Statistic Spectral Analysis of Pixel Hotspot

Measuring and analyzing the training samples of burned area, urban settlement, bare land and vegetation (bare land, forest, shrub, and plantation) from Himawari-8 performed by calculate statistic are minimum, maximum, average and standard deviation values of all band. The Normalized Distance (D) calculation used to analyze the potential of each band and discriminated between burned and unburned area (bare land, urban settlement, vegetation and water). The assessment is based on a discrimination index similar to the one proposed by Kaufman and Remer (1994).

$$D = \left| \frac{\mu f - \mu nf}{\sigma f + \sigma nf} \right| \quad (2\text{-}1)$$

D=Normalize Distance,
μ_f =mean of burned area
μ_{nf} =mean of unburned area,
σ_f =standard deviation of burned area,
σ_{nf} =standard deviation of unburned area

d. Data Validation

The data validation of data obtained from the visual interpretation by comparing the MODIS hotspot data overlay on data Himawari-8 and Landsat 8, which indicates the presence of burned area.

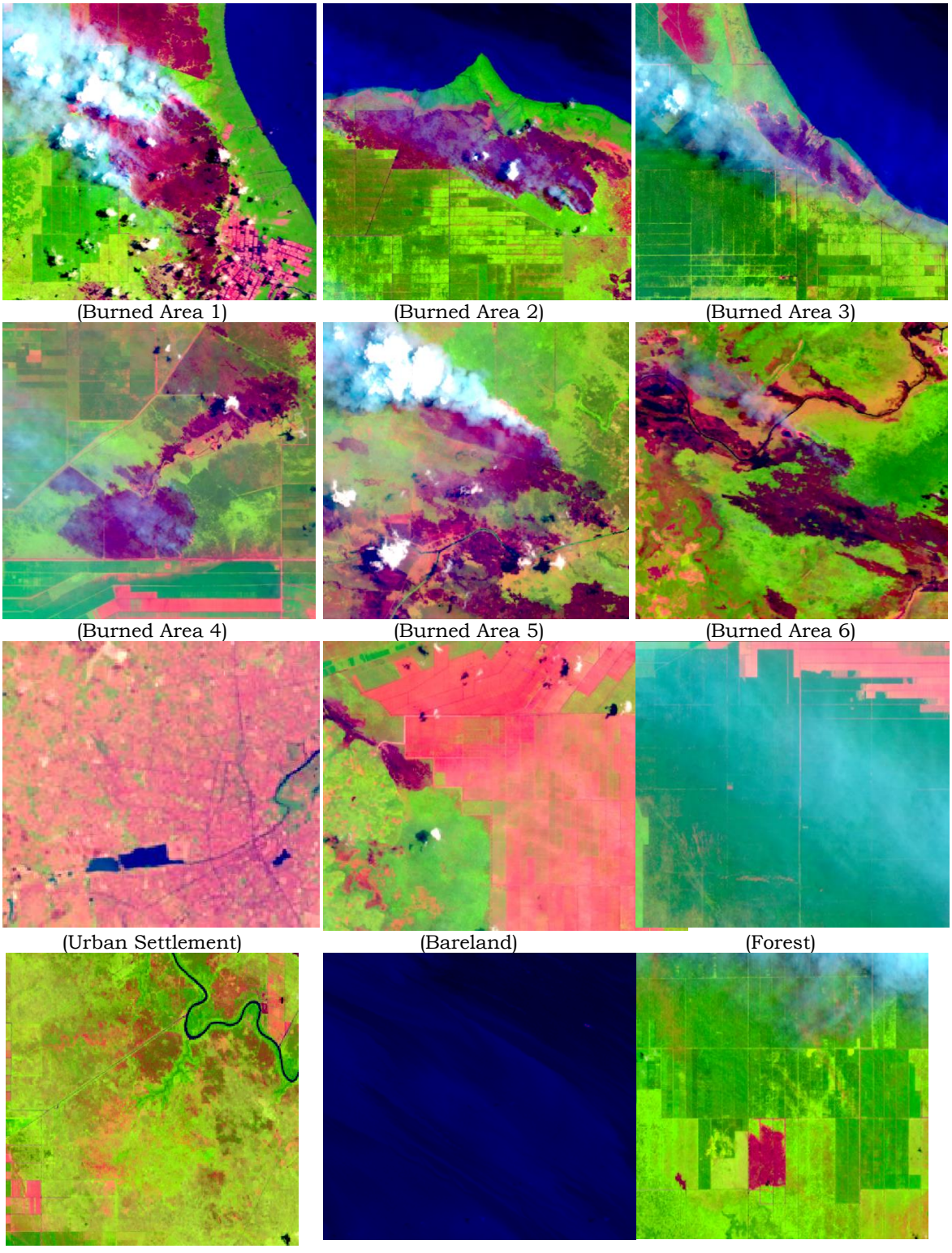

Figure 2-2: Training sample burned and unburned area for analysis. Selection of sample site is assisted with Landsat-8 image of natural color composite RGB 654 on September 23, 2015.

3 RESULT AND DISCUSSION

Some researches related to the benefit of Himawari-8 to detect the hotspot had already done by Fatkhuroyan *et al.* (2017) using the combination of band 3, 4, and 6 to detect the fires in Sumatera and Kalimantan. Meanwhile, Wickramasinghe *et al.* (2016) took the location in Fitzroy, Camballin, and Broome, Australia has been successful in mapping the boundaries of land fires with the unburned ones from forest fires based on red band pixel value, middle infrared, and infrared. As mention above, the spatial resolution of the band continued are 0.5 km, 1 km, and 2 km. Image with 0.5 km spatial resolution is very useful for the purposes of fire detection in Indonesia which has large varied sizes. Furthermore, beside its ability to detect fires and smokes, the use of this data is particularly suitable for on-site monitoring, since it has a high recording period (Hally *et al.* 2016).

According to hotspot detection from MODIS image using 4 μm (channel 21 or 22) and 11 μm channel (channel 31), the hotspot detection method of MODIS data is based on algorithm which is built for AVHRR and TRMM VIRS image data (Giglio *et al.* 1999; Justice *et al.* 1996; Kaufman *et al.* 1990: Kaufman *et al.* 1998, Justice *et al.* 2002; Giglio *et al.* 2003). It also uses red and near infrared channels with 250 m spatial resolution to remove fake hotspots due to *sun glint* (Justice *et al.* 2002). By considering the channels used to detect hotspots with MODIS data above, it can be seen that hotspots can be detected using 4μm, 11 μm, 0.86 μm and 0.65 μm wavelengths. In this research, sample training is taken for some burned and unburned objects such as vegetation (forests, plantations, and shrub), settlements, bare land and water shown by Figure 2-2. The performed of analysis is the extraction of reflectance value and Brightness Temperature (BT) to know the difference of characteristics of each objects in all bands. The results is obtained from the extraction of reflectance values on some objects are shown in Table 3-1 while for the BT value can be seen in Table 3-2.

Analyzed object data of Himawari 8 is adjusted to the Landsat-8 acquisition at 10:00. So that, according to analysis of spectral data pattern at 10.00, the burned area was shown by the red color in Figure 3-1. Generally, it can be distinguished from other objects they are settlement, vegetation, bare land and water particularly in band 1, band 2, and band 3. However, in band 3 the difference of burned area with other objects is very clearly visible, as well as for areas that are not burned visible differences in reflectance values in this band.

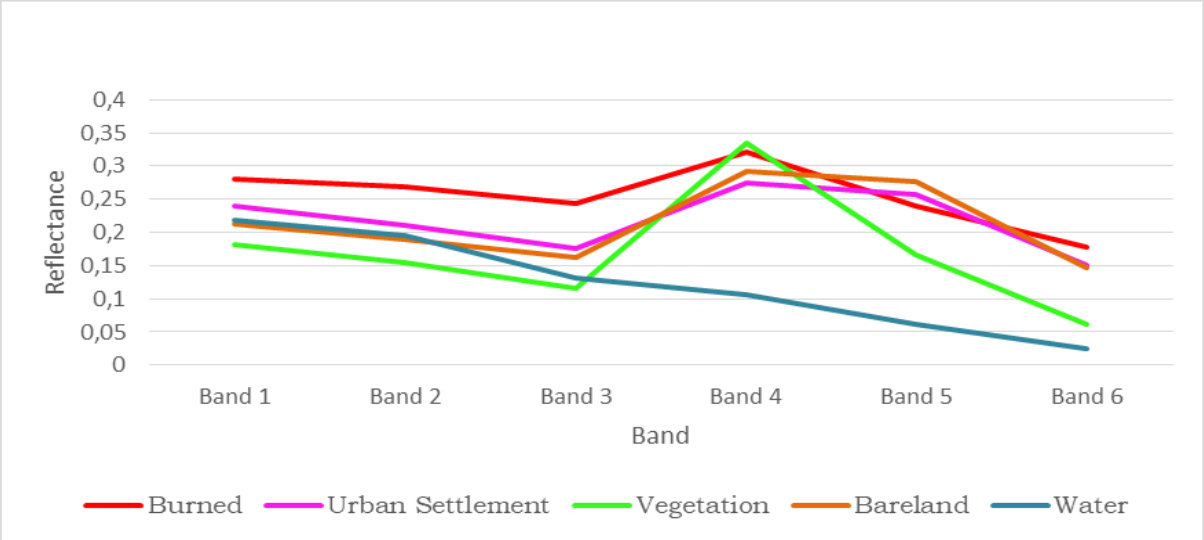

Figure 3-1: Spectral Patterns of burned and unburned objects

Table 3-1: The reflectance values of Burned and unburned objects
(Data on 23 September 2015, at 10:00 am)

	Burned					Settlement				
Band	**Min**	**Max**	**Mean**	**STD**	**CV**	**Min**	**Max**	**Mean**	**STD**	**CV**
1	0,16	0,36	0,28	0,06	0,20	0,23	0,24	0,24	0,01	0,02
2	0,14	0,38	0,27	0,07	0,25	0,20	0,22	0,21	0,01	0,02
3	0,10	0,38	0,24	0,08	0,33	0,16	0,19	0,18	0,01	0,05
4	0,21	0,44	0,32	0,06	0,19	0,25	0,28	0,27	0,01	0,04
5	0,17	0,28	0,24	0,03	0,13	0,23	0,28	0,26	0,02	0,07
6	0,07	0,29	0,18	0,07	0,38	0,12	0,17	0,15	0,02	0,14

Tabel 3-1: (Continued)

	Vegetation					Bareland					Water				
Band	Min	Max	Mean	STD	CV	Min	Max	Mean	STD	CV	Min	Max	Mean	STD	CV
1	0,15	0,29	0,18	0,04	0,19	0,17	0,29	0,21	0,04	0,17	0,21	0,23	0,22	0,01	0,03
2	0,12	0,26	0,16	0,03	0,21	0,15	0,26	0,19	0,03	0,17	0,18	0,21	0,20	0,01	0,04
3	0,09	0,22	0,12	0,03	0,26	0,13	0,21	0,16	0,02	0,15	0,11	0,16	0,13	0,01	0,10
4	0,28	0,40	0,33	0,04	0,11	0,25	0,36	0,29	0,03	0,09	0,07	0,29	0,11	0,07	0,64
5	0,13	0,22	0,17	0,03	0,17	0,19	0,32	0,28	0,05	0,19	0,03	0,24	0,06	0,06	1,05
6	0,05	0,09	0,06	0,01	0,19	0,09	0,18	0,15	0,03	0,21	0,01	0,11	0,03	0,03	1,24

When seen from Table 3-1 then band 4 for burned area has high reflectance value compared to other object but in band 4 reflectance object has value close to vegetation object, so for this band still difficult to distinguish between burned area with vegetation and then decreases in band 5 to band 6. The lowest of reflectance value is in band 6. Seeing from the pattern in Figure 3-1, the reflectance value in band 3 for the burned object separated with other objects, so that for the next band 3 is needed further to be analyzed.

The next analysis is the value of Brightness Temperature (BT). From Figure 3-2, it can be seen that burned objects in band 7 is different from other objects, while for the other band fire objects coincide with the other objects, i.e. settlement, vegetation, and bare land. In contrast, to the object of water although the near burned object yet still can be distinguished. The BT value on band 7 is the highest of all channels, while for band 8 and so on the BT value of the burned objects and other objects near together, mainly with residential objects and bare land. To distinguish it requires an advanced method of distinguishing burned objects by settlement or bare land since it has the same BT. The highest BT value of fire objects on band 7 is 340.99°K while the lowest BT value is bare land object on band 8 which is 239,57 °K (Tabel 3-2).

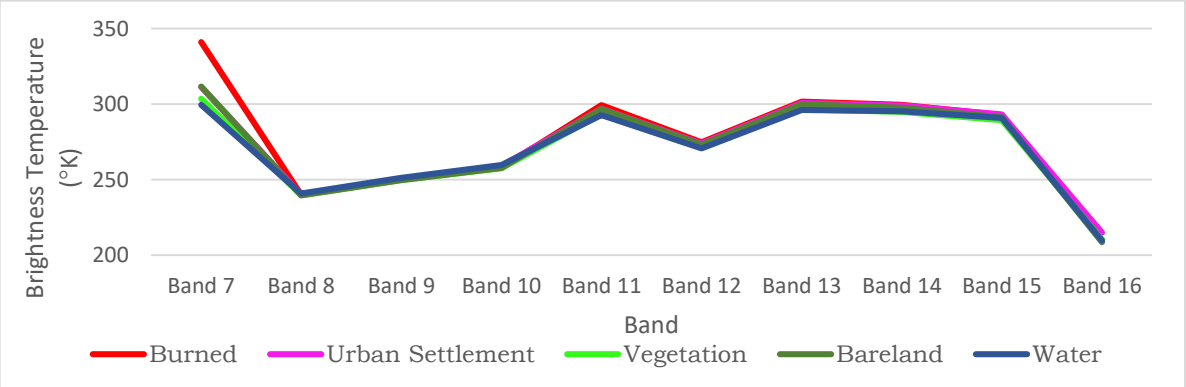

Figure 3-2: Brightness Temperature (BT) pattern of burned and unburned objects

Table 3-2: The value of Brightness Temperature (BT) burned and unburned objects (Data on September 23, 2015, at 10.00 am)

Class	Band 7	Band 8	Band 9	Band 10	Band 11	Band 12	Band 13	Band 14	Band 15
Burned	340.99	239.97	250.07	257.94	299.33	274.82	301.69	299.47	292.69
Settlement	311.34	240.14	250.63	258.99	296.96	273.77	300.88	299.19	293.24
Vegetation	303.59	239.68	249.64	257.55	293.356	271.01	296.62	294.79	289.38
Bare land	311.61	239.57	249.71	257.77	296.804	273.18	299.92	297.69	291.24
Water	299.53	240.83	251.24	259.02	292.714	270.62	296.19	295.38	290.87

Table 3-3: Normalized Distance value (D) reflectance (band 1-band 6) and brightness temperature (band 7-band 15)

	Normalized distance					
Class	Band 1	Band 2	Band 3	Band 4	Band 5	Band 6
Burned vs. Bare land	0.73	0.79	0.77	0.32	0.46	0.33
Burned vs. vegetation	1.08	1.14	1.15	0.14	1.24	1.47
Burned vs. water	0.97	0.97	1.20	1.67	1.89	1.56
Burned vs. urban settlement	0.68	0.81	1.20	0.65	0.40	0.32

Table 3-3: (Continued)

	Normalized distance								
Class	Band 7	Band 8	Band 9	Band 10	Band 11	Band 12	Band 13	Band 14	Band 15
Burned vs. Bare land	1.02	0.73	0.43	0.17	0.422	0.389	0.341	0.363	0.386
Burned vs. vegetation	1.34	0.45	0.50	0.42	0.942	0.934	0.929	0.857	0.831
Burned vs. water	1.44	1.91	1.89	2.67	1.102	1.018	1.035	0.772	0.503
Burned vs. urban settlement	1.09	0.31	0.90	1.49	0.448	0.295	0.183	0.063	0.180

Table 3-4: Coefficient Variant of reflectance (band 1-band 6) and brightness temperature (band 7- band 15)

	Coefficient Variant					
Class	Band 1	Band 2	Band 3	Band 4	Band 5	Band 6
Burned	0.203	0.250	0.329	0.187	0.126	0.376
Urban Settlement	0.021	0.024	0.045	0.044	0.066	0.140
Vegetation	0.192	0.206	0.259	0.108	0.168	0.194
Bare land	0.169	0.175	0.147	0.092	0.191	0.212
Water	0.032	0.036	0.099	0.636	1.049	1.240

Table 3-4: (Continued)

	Coefficient Variant								
Class	Band 7	Band 8	Band 9	Band 10	Band 11	Band 12	Band 13	Band 14	Band 15
Burned	0.077	0.002	0.002	0.002	0.016	0.012	0.013	0.013	0.010
Urban Settlement	0.003	0.001	0.000	0.001	0.002	0.001	0.001	0.001	0.001
Vegetation	0.006	0.001	0.001	0.002	0.005	0.003	0.005	0.005	0.004
Bare land	0.008	0.001	0.001	0.002	0.004	0.004	0.004	0.003	0.003
Water	0.009	0.000	0.000	0.000	0.004	0.003	0.004	0.004	0.003

The next analysis is the calculating separability or Normalized Distance (D) between the burning area and another objects. Based on the calculation of the value of D in Table 3-3 it can be seen that in general reflectance bands 1-6 are able to separate burned with vegetation but not sufficient for band 4. However, it has a low ability to separate burned with bare land and settlement. Burned objects can differentiate well by using BT in band 7 against bare land objects, vegetation, water and settlement, but it is difficult to distinguish between 8 - 15 bands burned with bare land and vegetation objects.

The last analysis is the calculation of coefficient variation value represents the ratio of the standard deviation to the mean. Based on the calculation of the value of CV (Coefficient Variation) in Table 3-4 it can be seen that in general reflectance bands 1-6 have good correlation for all class. According to Sugiyono (2007), interpretation the coefficient variation has level from very low until very strong. The value of low is 0.20 – 0.399 and very strong is 0.8 – 1.00. The high correlation compare another class identify by water in band 5 and band 6. Burned class area has value 0.3 identify has low variation.

4 CONCLUSION

According to the results of the analysis, it can be concluded that the Himawari-8 has good capability to identify land/forest fire hotspot as expressed for high accuracy assessment using band 3 and band 7. The pattern spectral data Himawari-8 using channel 3 (0.64µm) can distinguish the burned area with other objects. The highest Brightness Temperature value in the burned area can be identified from channel 7, and can be distinguished from other objects.

ACKNOWLEDGEMENT

This research was founded and facilitated by Remote Sensing Application Center of LAPAN. We would like to thank Japan Meteorological Agency has provided data access of Himawari-8 data. This research was presented at Seminar Nasional Penginderaan Jauh 2017.

REFERENCES

Bessho K., Date K., Hayashi M., *et al.*, (2016), An Introduction to Himawari-8/9-Japan's New Generation Geostationary Meteorological Satellites. Journal of the meteorological society of japan. Vol.94, No. 2, pp. 151-183.

Fatkhuroyan, Trinahwati, Panjaitan A., (2017), Forest Fire Detection in Indonesia using Satellite Himawari-8 (case study: Sumatera and Kalimantan on August-October 2015). IOP Conf. Series: Earth and Environment Science 54 012053. Doi:10.1088/1755-1315/54/1/ 012053.

Frankenberg E., McKee D., Thomas D., (2005), "Health Consequences of Forest Fires in Indonesia," Demography, 42(1): 109–129.

Giglio L., Kendall JD, Justice CO, (1999), Evaluation of global fire detection algorithms using simulated AVHRR infrared data. International Journal of Remote Sensing, 20, 1947–1985.

Giglio L., Descloitres J., Justice CO, *et al.*, (2003), An Enhanced Contextual Fire Detection Algorithm for MODIS. Remote Sensing of Environment, 273-283.

Hally B., Wallace LO, Reinke K., *et al.*, (2016), Assessment of the Utility of the Advanced Himawari Imager to Detect Active Fire Over Australia. The International Archies of the Photogrammetry, Remote Sensing and Spatial Information Sciences, Volume XL-I-88, 2016 XXIII ISPRS Congress. Prague, Chezch Republic.

Justice CO, Giglio L., Korontzi S., *et al.*, (2002), The MODIS Fire Product. Remote Sensing of Environment 83, 244-262.

Kaufman YJ, Tucker CJ, Fung I., (1990), Remote Sensing of Biomass burning in the tropics, J. Gephys, Res., 95, 9927-9939.

Kaufman YJ, Remer LA, (1994), Detection of forests using MID-IR reflectance: An application for aerosol studies. IEEE

Transactions on Geoscience and Remote Sensing, 32, 672−683.

Kaufman YJ, Justice CO, Flynn LP, *et al.*, (1998), Potential global fire monitoring from EOS-MODIS. Journal of Geophysical Research, 103, 32215– 32238.

Murdiyarso D., Lebel L., Gintings, *et al.*, (2004), Policy responses to complex environment problem: Insights from a Science-Policy Activity on Trans boundary Haze from Vegetation Fires in Southeast Asia. Agriculture Ecosystems & Environment 104(1):47-56. DOI: 10.1016/j.agee.2004.01.005.

Suwarsono, Rokhmatuloh, Tarsoen W., (2013), Pengembangan Model Identifikasi Daerah Bekas Kebakaran Hutan dan Lahan (Burned Area) menggunakan citra modis di Kalimantan. Jurnal Penginderaan Jauh Vol. 10 No. 2 Desember 2013: 93-112.

Sugiyono, (2009), Metode Penelitian Kuantitatif Kualitatif dan R&D. Bandung: Alfabeta.

Tacconi L., (2003), Kebakaran Hutan di Indonesia: Penyebab, Biaya dan Implikasi Kebijakan. Center for International Forestry Research. ISSN 0854-9818.

Wickramasinghe C., Jones S., Reinke K., *et al.*, (2016), Development of a Multi-Spatial Resolution Approach the Surveillance of Active Fire Lines Using Himawari-8. Remote Sensing, 8, 932.